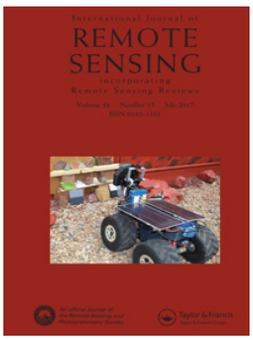

International Journal of Remote Sensing

ISSN: 0143-1161 (Print) 1366-5901 (Online) Journal homepage: https://www.tandfonline.com/loi/tres20

Identification of possible source areas of stone raw materials combining remote sensing and petrography

Hakan Tanyaş, Murat Dirican, M. Lütfi Süzen, Asuman G. Türkmenoğlu, Çağıl Kolat & Çiğdem Atakuman

To cite this article: Hakan Tanyaş, Murat Dirican, M. Lütfi Süzen, Asuman G. Türkmenoğlu, Çağıl Kolat & Çiğdem Atakuman (2017) Identification of possible source areas of stone raw materials combining remote sensing and petrography, International Journal of Remote Sensing, 38:13, 3923-3942, DOI: 10.1080/01431161.2017.1312032

To link to this article: https://doi.org/10.1080/01431161.2017.1312032

Published online: 30 Mar 2017.

INTERNATIONAL JOURNAL OF REMOTE SENSING, 2017
VOL. 38, NO. 13, 3923–3942
http://dx.doi.org/10.1080/01431161.2017.1312032

Taylor & Francis
Taylor & Francis Group

Identification of possible source areas of stone raw materials combining remote sensing and petrography

Hakan Tanyaş[a]*, Murat Dirican[b], M. Lütfi Süzen[a], Asuman G. Türkmenoğlu[a], Çağıl Kolat[c] and Çiğdem Atakuman[d]

[a]Geological Engineering Department, Middle East Technical University, Ankara, Turkey; [b]Department of Archaeometry, Middle East Technical University, Ankara, Turkey; [c]R&D Branch, Verisis Co., Ankara, Turkey; [d]Department of Settlement Archaeology, Middle East Technical University, Ankara, Turkey

ABSTRACT

Understanding the location and distribution of raw materials used in the production of prehistoric artefacts is a significant part of archaeological research that aims to understand the interregional interaction patterns in the past. The aim of this study is to explore the regional locations of the source rock utilized in the production of stone bowls, which were unearthed at the Neolithic (approximately 6500–5500 BC) site of Domuztepe (Kahramanmaraş-Turkey), via a combination of remote-sensing methods, petrographic and chemical analyses. To accomplish this task, the stone bowls were identified mineralogically, geochemically and spectrally, and then mapped with Advanced Spaceborne Thermal Emission and Reflection Radiometer (ASTER) sensors. According to the defined mineralogical composition, which is iron-rich chlorite, the target areas were selected among geologically potential areas that would bear similar source rocks in near vicinity and the target spectral signature was searched within these target areas. In order to overcome the problem of spectral similarity of chlorite group to some other minerals such as carbonate or epidote group minerals, band ratioing (BR) and feature-oriented principal component analysis (FOPCA) were used with an integrated approach and then their results were filtered according to the outcomes of the relative absorption band-depth (RBD) images. The areas with highest potentials were vectorized and then field checked. Mineralogical investigations on the collected field samples reveal that there is a mineralogical match between the source and target material. One group of stone bowls samples have similar geochemical signatures as the field samples having ultramafic origins. However, there is another group of stone bowls samples which are geochemically dissimilar to the first group of field and bowls samples. The data regarding the geochemical signatures of these two groups indicate a genetic relation between the sample sets. Therefore, it is concluded that the source rock of a major portion of the stone bowls unearthed at Domuztepe most probably originated from the near vicinity of the site.

ARTICLE HISTORY
Received 26 September 2016
Accepted 20 March 2017

CONTACT Hakan Tanyaş h.tanyas@utwente.nl Geological Engineering Department, Middle East Technical University, Ankara, Turkey

*Present address: Faculty of Geo-Information Sciences and Earth Observation (ITC), University of Twente, Enschede, The Netherlands.

1. Introduction

Remote sensing is a widely used complementary tool that has vast applications in a variety of areas. Archaeological studies are part of these areas and moreover remotely sensed data were employed by the archaeological community into their research relatively early in comparison with other disciplines (Sever 1995). In fact, by using aerial photography, archaeology was one of the first disciplines to apply remote-sensing technology at the turn of the twentieth century (Williamson and Nickens 2000). It had limited application areas at first and it was basically used for the detection of archaeological sites which were partially or totally buried, or in any case not visible from the ground (Orlando and de Villa 2011). However, it has become a commonly used tool in archaeology with time and with the rise of high spatial resolution satellites in the past decade providing the detection or even the direct visualization of archaeological manifestations (e.g. Lasaponara and Masini 2009; Parcak 2009). Satellite spectral remote sensing is not fully utilized in the archaeological community.

Today, a number of airborne and satellite spectral sensing systems are available for remote-sensing applications (Cudahy et al. 2008). Among them, the advent of the Advanced Spaceborne Thermal Emission and Reflectance Radiometer (ASTER) has led to advances in mineral surface mapping with a complete coverage of the Earth's land surface for 14 spectral bands (Cudahy et al. 2008). It also possesses sufficient spectral resolution in the shortwave infrared (SWIR) for mapping hydrothermal alteration minerals (Pour and Hashim 2012). Chlorite is one of these minerals. Propylitically altered rocks contain varying amounts of chlorite (Salisbury 1983; Rowan, Schmidt, and Mars 2006; Clark et al. 2007; Brandmeier et al. 2013) and they characterize the margins of porphyry copper deposits as well as epithermal precious metal ores (Robb 2013). In that sense, chlorite can be considered as a substantially important mineral especially with respect to the exploration of ore deposits. Moreover, it has also special importance in the scope of this study since it constitutes the raw material of a remarkable number of artefacts found at the Later Neolithic site of Domuztepe.

The site of Domuztepe (Kahramanmaraş, Turkey) represents the Northwestern border of a unique material culture distribution commonly known as the Halaf culture (Campbell et al. 1999; Carter, Campbell, and Gauld 2003) which had influenced vast regions of Northern Mesopotamia during the final stages of the Later Neolithic time period (approximately 6500–5500 BC). Domuztepe remains of the largest known Halaf period sites (at 20 ha in total area) in all of the ancient Near East (Campbell et al. 1999). If the whole site was engaged simultaneously, as suspected by the excavators, at least for the later phases of the site, the population may have been as high as 1500 people, substantially larger than any other known Halaf – Chalcolithic site in Anatolia or contemporary Mesopotamia (Kansa et al. 2009). The Halaf culture is traditionally defined through its elaborately painted pottery, stone bowls, as well as a number of other portable artefacts, which have long been speculated to originate from a centre in Northern Iraq. However, the material unearthed at Domuztepe has provided evidence that a single centre in Northern Iraq may no longer be a viable explanation for the Halaf material culture distribution. Whereas an important portion of the ceramics and other artefacts unearthed at Domuztepe show close stylistic affinities with the artefacts found in other parts of Northern Mesopotamia, the very same artefacts are also observed to be

an integral part of independent traditions of local production. Within this context, understanding the raw material location, use, and distribution at local and interregional scales has been an important research question at Domuztepe (Campbell and Carter 1998). Whereas the stylistic analyses of stone bowls is an ongoing research at Domuztepe (Campbell 2012), this study is particularly focused on locating the raw material sources utilized in the production of stone bowls at the vicinity of Domuztepe via a combination of remote-sensing methods and petrographic and chemical analyses.

At the beginning of this study, field surveys and sampling were conducted within the exposures of ophiolitic melange in the near vicinity of the study area to locate the possible source areas of the chlorite-rich raw materials used to manufacture stone bowls recovered at the Domuztepe site. However, the source material of stone bowls could not be found. Since the area covered by potential source rocks has a large extend, the remote-sensing techniques were employed and the target areas for the field work and sampling were determined. During the second phase of the investigation, laboratory studies were conducted to understand the mineralogical and chemical characteristics for the field and stone bowl samples for provenance analysis and to locate source rock exposures exploited to manufacture stone bowl artefacts.

2. Study area and data set

Domuztepe is located at the southeastern part of Turkey within the municipal boundary of Kahramanmaraş city. The region is characterized by a nearly semi-arid climate. It is about 40 km south of the Kahramanmaraş city centre and located between the Cennetpınarı and Emiroğlu villages (Figure 1). The Kahramanmaraş plain drained by Aksu stream that the Domuztepe site is located appears as a geographical connection area which is extended by Cilicia and Mediterranean basins at the west, Amik plain at the south, Anatolia plateau at the north and flat plains of Syria and Mesopotamia at the east. The study area, which is also within the southeast Anatolian orogenic belt, comprises different tectonic units with various lithological sequences (Yilmaz, Over, and Ozden 2006) (Figure 2). Among these units, ophiolites are considered as primary target areas for the source rock of stone bowls.

The dataset used in this study include two level 1B ASTER images with ASTL1B0030916200208282910102002081100 and ASTL1B0031021200308265 71-1032003093317Granule IDs (Table 1) and the geological map of the area is prepared by the General Directorate of Mineral Research and Exploration (MTA 2004).

3. Methodology

In the scope of this study, thin sections were prepared from stone bowls and field samples for mineralogical investigations. The petrographical examination of thin sections is accompanied by X-ray powder diffraction analysis of the samples in order to identify minerals. Based on the mineralogical investigations the significant mineral component of stone bowls was defined as iron-rich chlorite. Same samples were also identified spectrally via field spectrometer. After reaching the representative spectral signature of unearthed material, areas having similar spectral signature were searched in the near vicinity of the

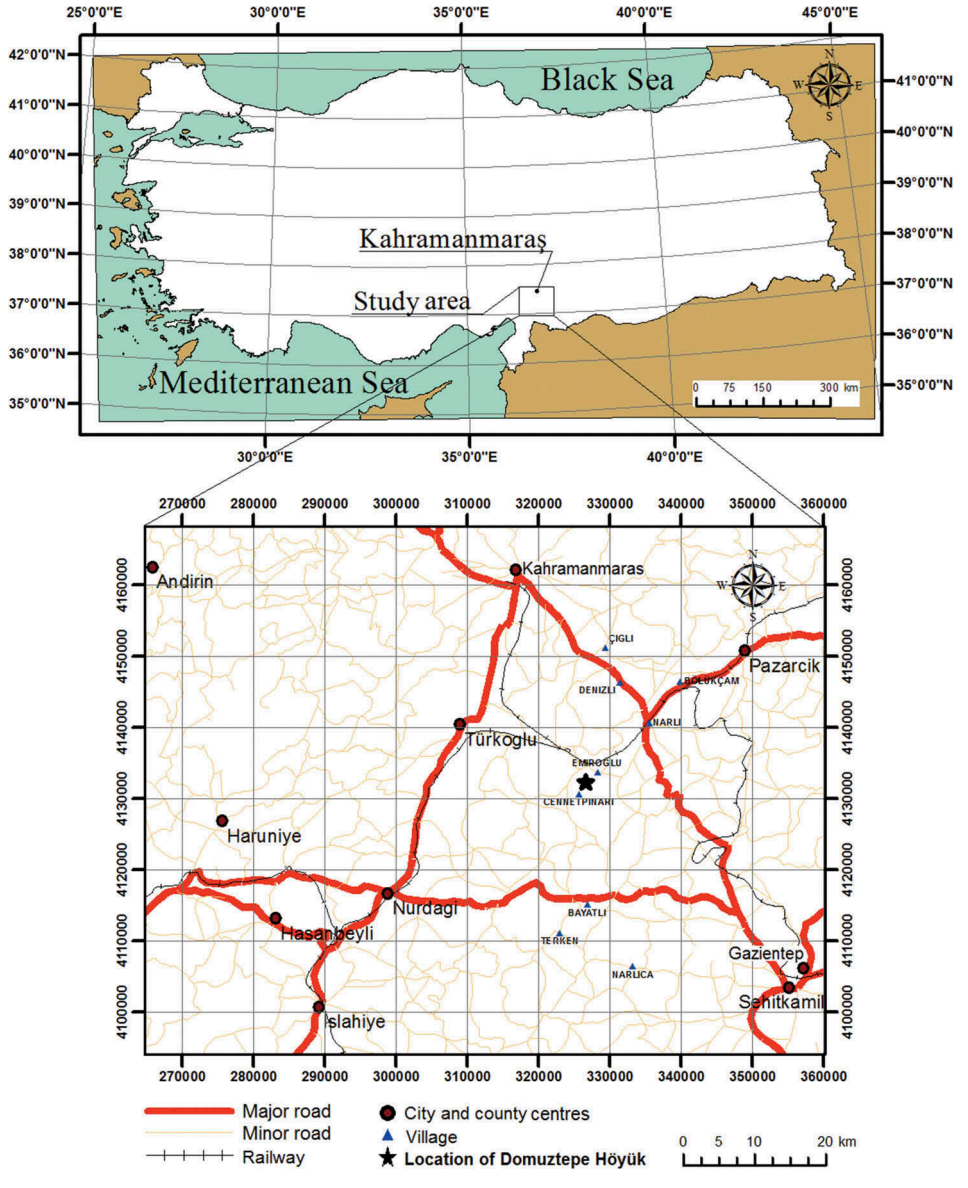

Figure 1. Location of the study area.

study area. In order to limit the extent of surveying area, the locations of ophiolitic units which are the most possible source rocks for iron-rich chlorite, located in the near vicinity of the study area were defined from regional geological maps. The remote-sensing applications hereupon were conducted for the area covered by ophiolitic units (Figure 2). Thereafter, cloud-free ASTER images for the study area were acquired. According to the target spectral signature, images were subjected to the combined version of two different spectral enhancement techniques which are (i) band ratioing (BR) and (ii) feature-oriented principal component analysis (FOPCA), and then the results

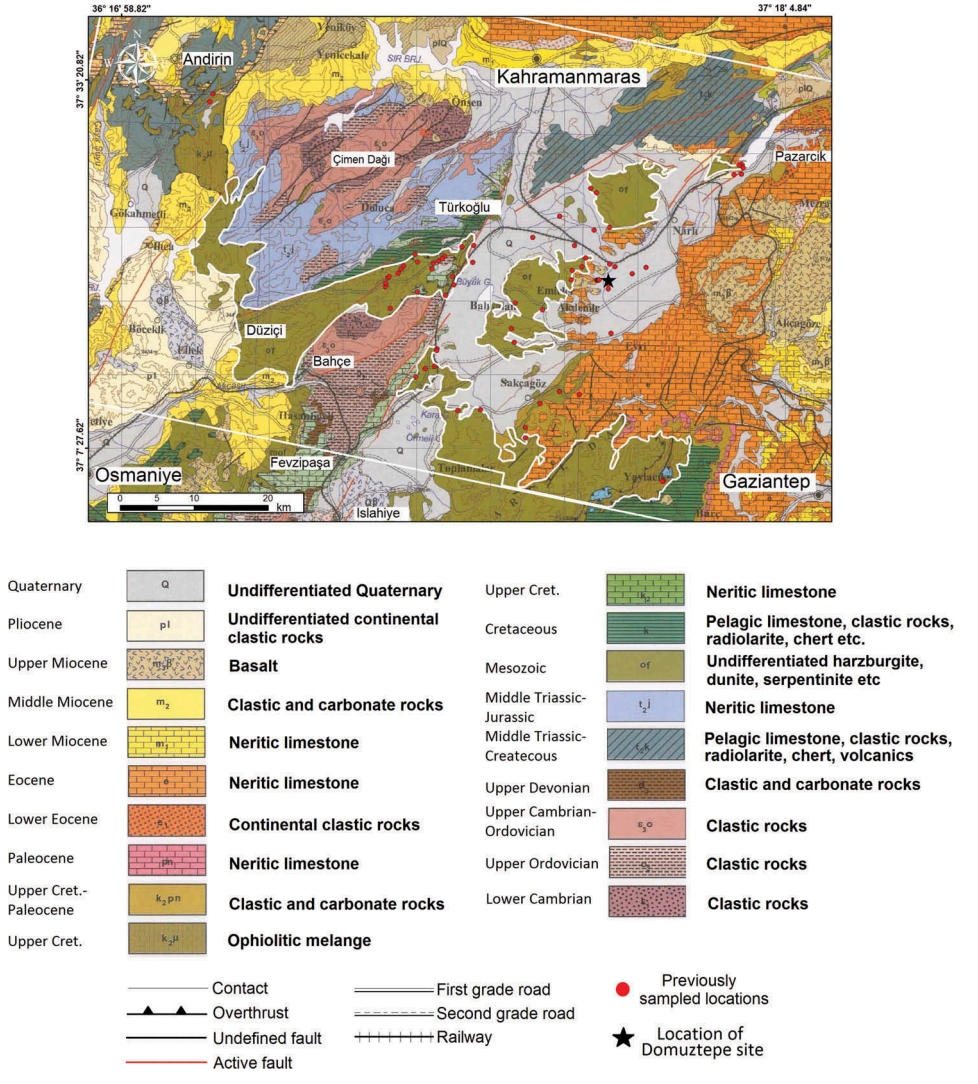

Figure 2. Geology of the study area and its surrounding region (white lines indicate the footprint of Figures 3(*a*) and (*b*)) (MTA 2004).

were refined with (iii) the relative absorption band-depth (RBD) approach. The results of these analyses were evaluated together and the areas with the highest probabilities were vectorized. In the final stage of the study, a field survey was conducted in order to check the validity of remote-sensing products and sampling was carried out at the defined locations. Mineralogical investigations for defining the composition of these collected field samples were also conducted on thin sections.

3.1. *Pre-processing*

The cloud-free ASTER images, gathered for this study, were subjected to some pre-processing operations which are registering, masking and atmospheric correction. The spectral

Table 1. Detailed information about the Advanced Spaceborne Thermal Emission and Reflection Radiometer (ASTER) scenes used.

Scene information type	Value	
Granule ID	ASTL1B 0209160828290210100006	ASTL1B 0310210826570311030417
Processing level	1B	1B
Acquisition date	9 October 2002	2 November 2003
Source data product	ASTL1A 0209160828290210090547	ASTL1A 0310210826570311020083
Scene centre	37° 17' 44.977" N, 37° 18' 32.061" E	37° 23' 43.645" N, 36° 37' 25.071" E
Scene upper left	37° 38' 8.6856" N, 36° 57' 29.044" E	37° 43' 59.538" N, 36° 16' 9.4836" E
Scene upper right	37° 30' 44.686" N, 37° 47' 22.160" E	37° 36" 53.251" N, 37° 06' 9.8712" E
Scene lower right	36° 57' 16.668" N, 37° 39' 24.148" E	37° 03' 22.968" N, 36° 58' 29.629" E
Scene upper left	37° 04" 37.963" N, 36° 49' 52.575" E	37° 10" 26.875" N, 36° 08' 51.093" E
Solar direction	156^0 04' 8.1372" N, 53^0 01' 12.752" E	163^0 36' 9.450" N, 40^0 33' 42.746" E

analysis was carried out using TNTmips® Pro (MicroImages 1997) and ENVI 4.8® (ITT 2010) software. Firstly, acquired ASTER images with radiometric and geometric corrections corresponding to level 1B (Abrams, Hook, and Ramachandran 2002) were registered to Universal Transverse Mercator (UTM) Zone 37 World Geodetic System (WGS) 84. Afterward, crosstalk effect was checked according to the report of Cudahy et al. (2002) but effects of any energy overspill from band 4 into bands 5 and 9 were not detected. In the subsequent stage, 30 m SWIR data were resampled into 15 m visible and near-infrared (VNIR) data in both datasets. The images were atmospherically corrected and VNIR and SWIR bands of the data were converted to reflectance using the internal average relative reflectance (IARR) (Ben-Dor et al. 1995) method. Finally, based on the geological map of the study area (Figure 2) a mask was created to filter the areas of outcropping ophiolitic units only. The false colour image and the ophiolitic outcrop mask are presented in Figures 3(*a*) and (*b*).

3.2. *Spectral properties of iron-rich chlorite*

A total of 47 samples representing the stone bowls were investigated by a field spectrometer and spectral signature of the material was defined as chlorite (Figure 4), in coherence with the mineralogical/petrographical analyses.

Laboratory studies have shown that most of the major rock-forming minerals have spectral reflectance curves with diagnostic absorption features (Cudahy et al. 2008). Electronic and vibrational processes within the mineral crystal lattice are the causes for these absorption features (Prost 2013) which serve important characteristics to differentiate minerals based on remote-sensing techniques.

There are many studies aimed to map alteration minerals including chlorite (e.g. Rowan et al. 2003; Dalton et al. 2004; Rowan, Schmidt, and Mars 2006; Bishop et al. 2008) because of its role in the exploration of ore deposits. However, due to the overlapping spectral absorption features, discrimination and identification of chlorite minerals require special effort (Dalton et al. 2004) especially while working with ASTER images.

Reflectance spectra of chlorites have hydroxyl absorption features (Fe–OH) in SWIR region of the electromagnetic spectra (Brandmeier et al. 2013). While the sharp and well resolved OH combination bands in the 2350–2370 nm region provide unique fingerprints as absorption, the weak H–O–H combination bands are observed near 2000 nm for adsorbed water in spectra of the chlorites (Bishop et al. 2008) (Figure 5). However, the spectral behaviour of chlorite shows similarities with some other phyllosillicate

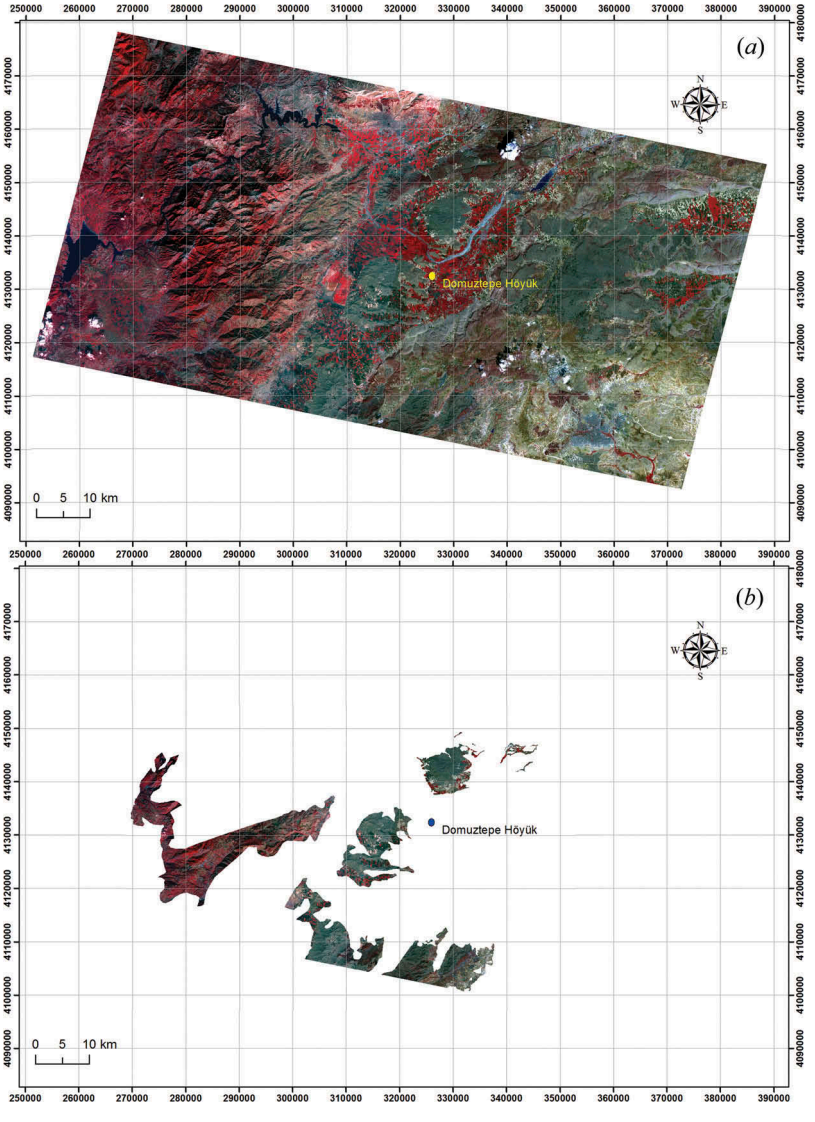

Figure 3. (*a*) False colour image (432/RGB) and (*b*) the residual area after masking geological units different than ophiolitic units.

minerals (smectites, kaolinite-serpentines, and micas) (Bishop et al. 2008) and also some other alteration minerals (calcite and epidote) (Dalton et al. 2004) (Figure 5). Therefore, in order to discriminate the iron-rich chlorite from its environment, more than one spectral enhancement techniques are required to be applied.

3.3. *Image processing and mapping iron-rich chlorite*

3.3.1. *Band ratioing (BR)*

BR process is performed by dividing numerical values in one band by those in another for each pixel in order to enhance variations in the slopes of the spectral reflectance

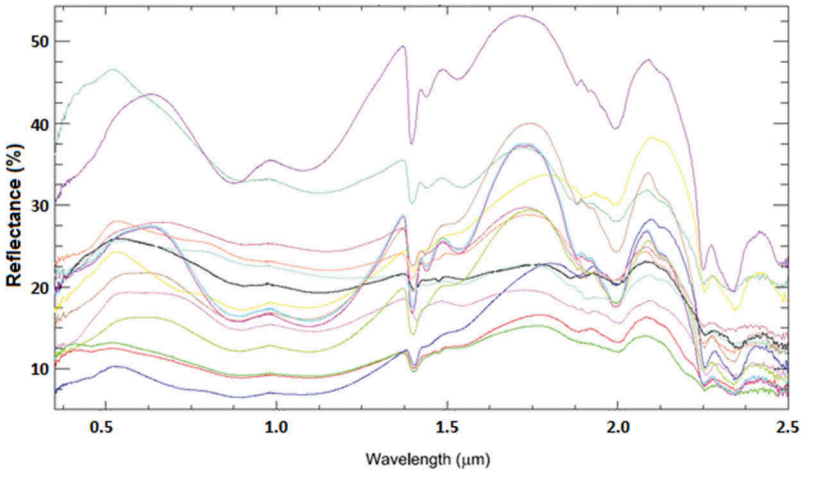

Figure 4. Reflectance spectra of samples prepared from stone bowls.

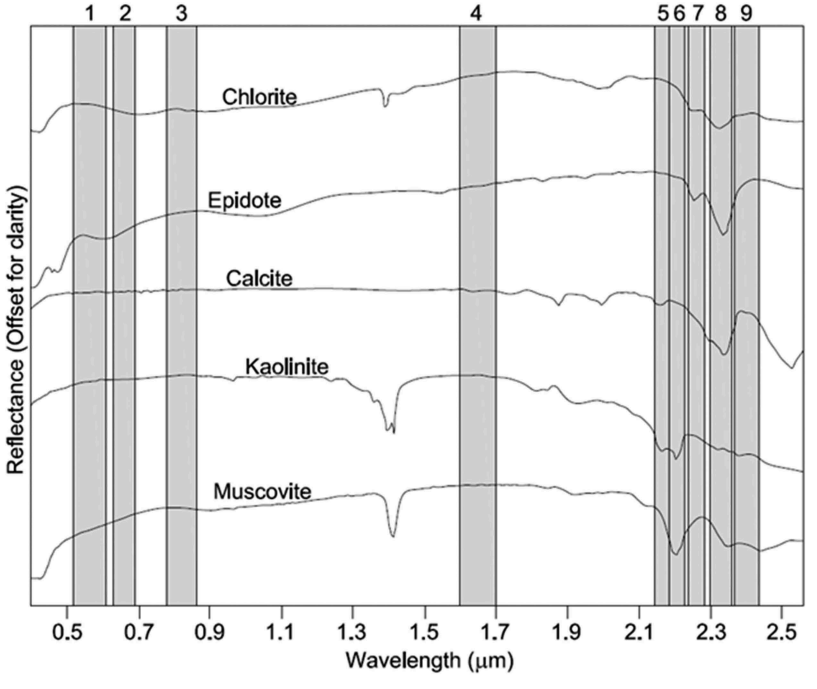

Figure 5. Laboratory reflectance spectra of chlorite and some other alteration minerals (USGS Spectral Library). The numbers given at the top indicate the corresponding Advanced Spaceborne Thermal Emission and Reflection Radiometer (ASTER) bands.

curves between the two different spectral ranges in the resultant image (Öztan and Süzen 2011).

According to the spectral reflectance curve of the chlorite (Figure 5), the features observed in the VNIR region can be used to eliminate some of the overlaps between the

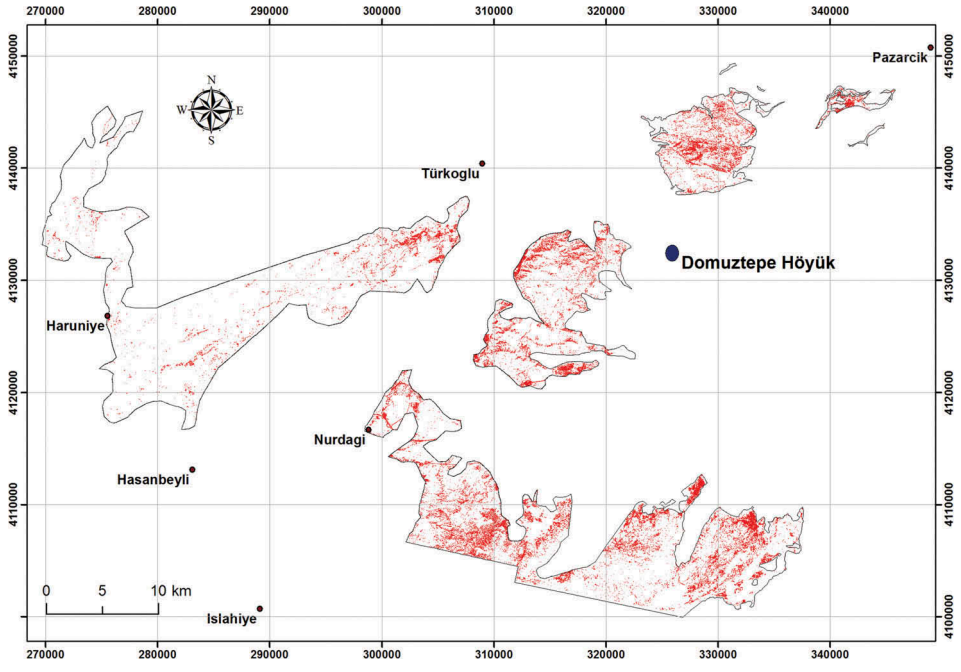

Figure 6. Areas satisfying the defined band ratioing (BR) conditions.

chlorite and some other alteration minerals. The observations regarding the spectral behaviour of iron-rich chlorite in this region (Figures 4 and 5) reveal that ASTER band 1 and 2 give close reflectance in this region, while band 2 gives high reflectance comparing to the band 3. In order to assess the success of the band ratios and make a further comparison with the field observation, some thresholds should be set (Öztan and Süzen 2011). Thus, the following thresholds were applied on the defined band ratios:

$$1.1 > (R_{\text{band1}}{:}R_{\text{band2}}) > 0.9 \text{ and } (R_{\text{band2}}{:}R_{\text{band3}}) > 1,$$

where R represents the reflectance. Areas satisfying these conditions are presented in Figure 6.

3.3.2. *Feature-oriented principal component analysis (FOPCA)*

FOPCA technique was developed by Loughlin in 1991 as a modified version of feature-orientated principal component selection (FPCS) (Crosta and Moore 1990). It is based on the idea of establishing the relationship between the spectral responses of target materials numeric values extracted from the eigenvector matrix used to calculate the principal component (PC) images. During this operation, the specific bands are selected as an input of FOPCA to ensure that certain materials would not be mapped and that spectral information due to target materials (alteration minerals) would be mapped into a single PC (Öztan and Süzen 2011). The bands are selected in a way to resemble the spectral signature of the target material with two reflections and two absorption bands (Crosta et al. 2003). According to the defined method, the ASTER band 4 and 5 were selected as ones with high reflection and bands 7 and 8 were selected as absorption reflected feature (Figures 4 and 5). FOPCA technique was applied on each contiguous geographic outcrop

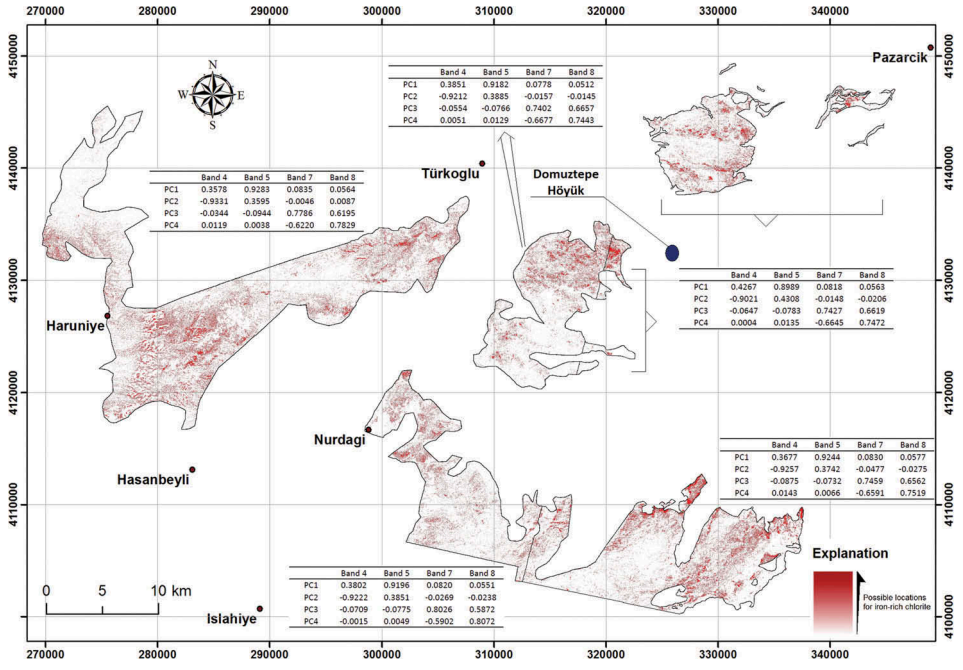

Figure 7. Feature-oriented principal component analysis (FOPCA) result with related eigenvectors of the covariance matrix.

of ophiolitic units separately in order to increase the enhancement power of the method (Figure 7). As a result of FOPCA, the eigenvector statistics were obtained and examined for each portion. The observations indicate that PC3 has negative loading from band 4 and 5 and positive loading from band 7 and 8, indicating that pixels likely to contain iron-rich chlorite will be represented by low (dark) digital numbers (DNs) in PC3 for each portion (Figure 7). The appropriate threshold value for PCA3 was also selected to filter the most potential areas, and the resultant image is presented in Figure 7.

3.3.3. *Combining the BR and FOPCA*

After obtaining these results, they were combined in a way that their outputs were not lost while information from both maps was delineated in a more refined way. The result of this analysis was represented by binary raster files. In the resultant BR image, 0 was assigned to the areas that do not satisfy the criterion and 1 was assigned to the satisfying areas, while for the FOPCA, 10 was assigned to the satisfying area and 0 was assigned to the unsatisfactory results (Figure 8). Overall, cells with 11 were considered as the most probable area containing iron-rich chlorite based on the result of BR and FOPCA (see inset of Figure 8 for possible scores and their explanations) (Figure 8).

3.3.4. *Relative Absorption Band-Depth (RBD)*

RBD (Crowley, Brickey, and Rowan 1989) images provide useful three-point ratio formulation for displaying Al–O–H, Fe, Mg–O–H absorption intensities (Pazand, Sarvestani, and Ravasan 2013). In this study, RBD images were produced for iron chlorite and muscovite/sericite group minerals and thereafter, a colour composite was created

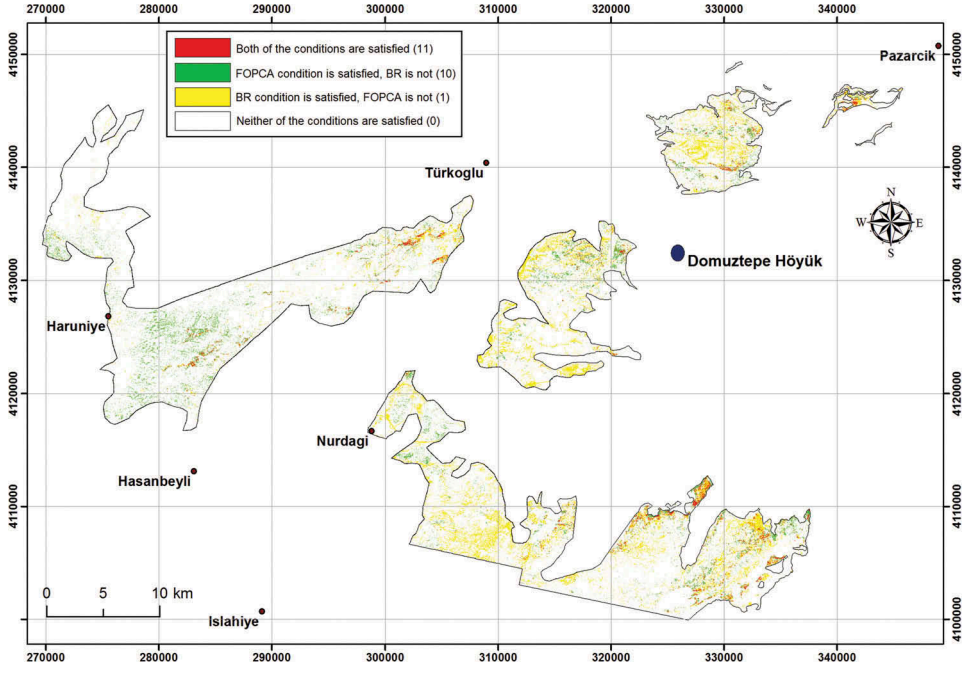

Figure 8. Result of combined evaluation of both BR and FOPCA.

accordingly (Figure 9). The RBD image which is sensitive against muscovite/sericite was used to discriminate them from the rest of target area. As a result of visual observations, the possible locations were detected and they were identified according to their priority order as T1–T8 (Figure 9).

3.3.5. *Synthesis*

As a final stage of remote-sensing processes conducted in the study area, the matches between the areas detected by BR /FOPCA and RBD were checked (Figure 10). A perfect match was obtained in the target 1, 2, 3, and 4 while some matches were also obtained in target 6 and 8, although they are not so strong. In target area number 5 and 7 in contrast to the result of RBD, BR /FOPCA did not give any signature regarding the existence of iron-rich chlorite mineral. Therefore, these locations are eliminated from further investigations.

4. Mineralogical and geochemical evaluation of target results

As shown in the previous sections the target areas 1, 2, 3, and 4 which are identified by means of remote-sensing data processing, give the best signature regarding the possible existence of rocks enriched in iron-rich chlorite mineral. Since these target areas are not included within the 'previously sampled locations' as shown in Figure 1, new field samples are collected from the target areas 1, 2, 3, and 4 which lie within the ophiolitic units exposed in the study area. In this way the ground truth for the remote-sensing data for the possible existence of unique chlorite-rich rock outcrops which might be the sources of chlorite-rich stone bowl artefacts collected at the Domuztepe archaeological site.

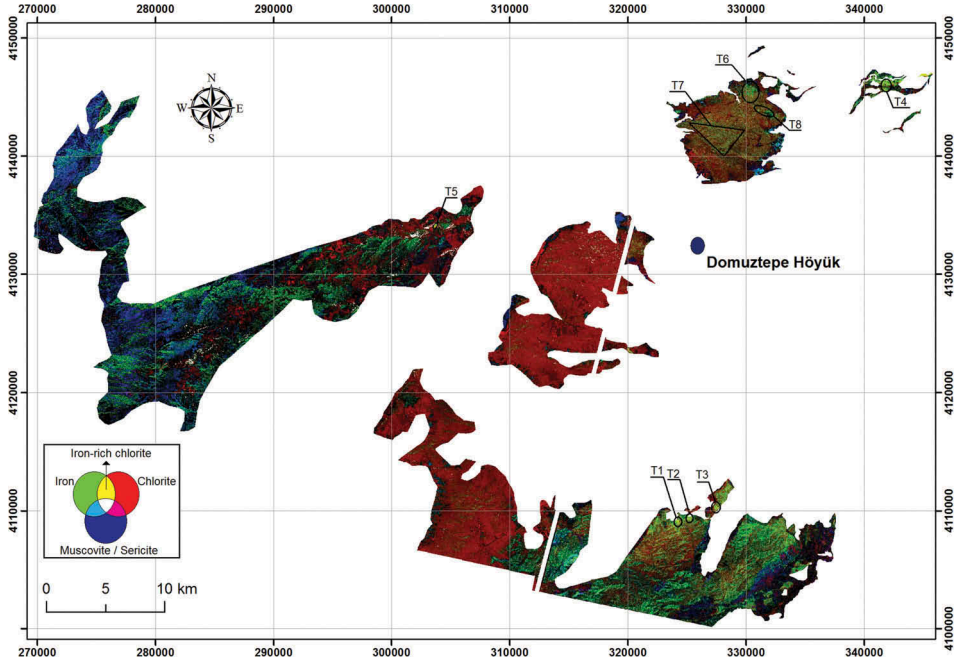

Figure 9. Colour composite created by relative absorption band-depth (RBD) images.

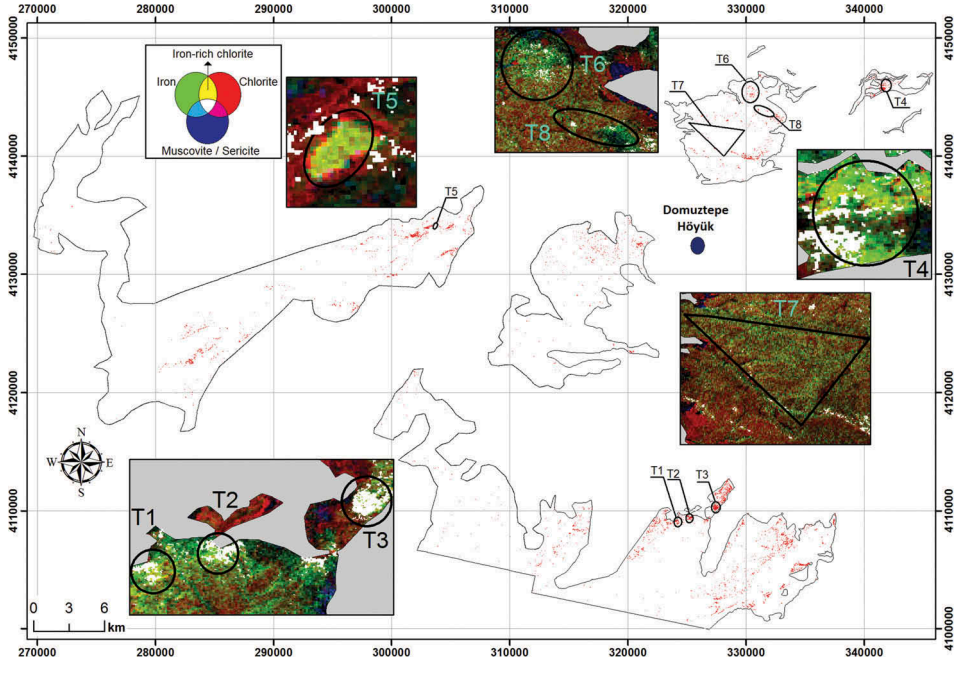

Figure 10. Target areas determined as a result of BR /FOPCA and RBD processes.

During this study, 47 stone bowl samples are analysed. The samples are obtained from Kahramanmaraş Museum by official permission. On the other hand, a total of 90 field samples are collected from different target areas in order to search for possible source areas for the raw materials of stone bowls. The mineralogical-petrographical properties and the geochemical characteristics of both the field samples and stone bowl artefacts are investigated by means of petrographic thin sectioning (PTS), X-ray powder diffraction analysis (XRD), and inductively coupled plasma-mass spectrometer (ICP-MS). Thin sections are studied by using Olympus BH2 microscope, equipped with an Olympus DP-10 digital camera available at the laboratories of the Geological Engineering Department of the Middle East Technical University (METU). A Philips Panalytical X'Pert PRO X-Ray Diffractometer at the laboratory of the Mineral Research & Exploration General Directorate (MTA) is utilized to obtain the diffraction patterns (diffractograms) of bulk samples and their clay fractions (<2 μm) by using Cu Kα radiation at 45 kV and 40 mA. The software program HighScore Plus used to assist the mineralogical identifications. The powdered bulk samples are sieved below 170 mesh sieve. These powders are used to identify minerals present in the rock samples in the search for the provenance of stone bowl samples. Geochemical analyses by ICP-MS analysis are performed by ACME Analytical Laboratories in Canada. Total rock analyses include sample preparation and the identification of the major, minor, trace and rare earth element concentrations in the rock samples. In this article, mainly the trace and rare earth elements are used to discriminate and match the petrographic groups of the field and stone bowl samples.

Petrographically, the archaeological stone bowl samples from Domuztepe site mainly form two groups; the first group consists of green coloured rocks rich in chlorite showing intensive violet pleochroism in thin section (Figures 11(*a*)–(*c*)). The identification of a Fe-rich chlorite composition is possible by XRD analysis of the bulk samples, based on the observation that odd order peak intensities (14 and 4.7 Å) are weaker compared to the even order reflections (7 Å) since the Fe content of chlorite mineral is known to increase relative to its Mg content (Figure 11(*d*)) (Moore and Reynolds 1997). Contrastingly, the second group is made of raw materials with few chlorite minerals but rather rich in serpentine. In some samples, in addition to serpentine mineral, pyroxene, olivine, black coloured opaque mineral and sphene can be identified besides some chlorite so that the precursor rock type in this group can be suggested as an ultramafic igneous rock. In the first group of rocks as mentioned above, the alteration in the form of chloritization is so intensive that the identification of their precursor rock is hardly possible as a mafic (gabbroic-basaltic) igneous rock.

Petrographically, the field samples show similar structural and textural properties in thin section (Figures 11(*e*)–(*g*)). Their dominant alteration product belongs to serpentine group minerals (predominantly antigorite). The existence of serpentine group minerals is also verified by the X-ray powder diffraction patterns (Figure 11(*h*)). Petrographic investigation indicates that the collected field samples are serpentinized ultramafic rocks.

The data collected from petrographic and XRD investigations of the stone bowl and field samples are if further compared with the chemical data obtained by ICP-MS analysis which will be used also to discriminate the groups of the Stone bowls based on their chemical properties and also to correlate them with those of field samples for

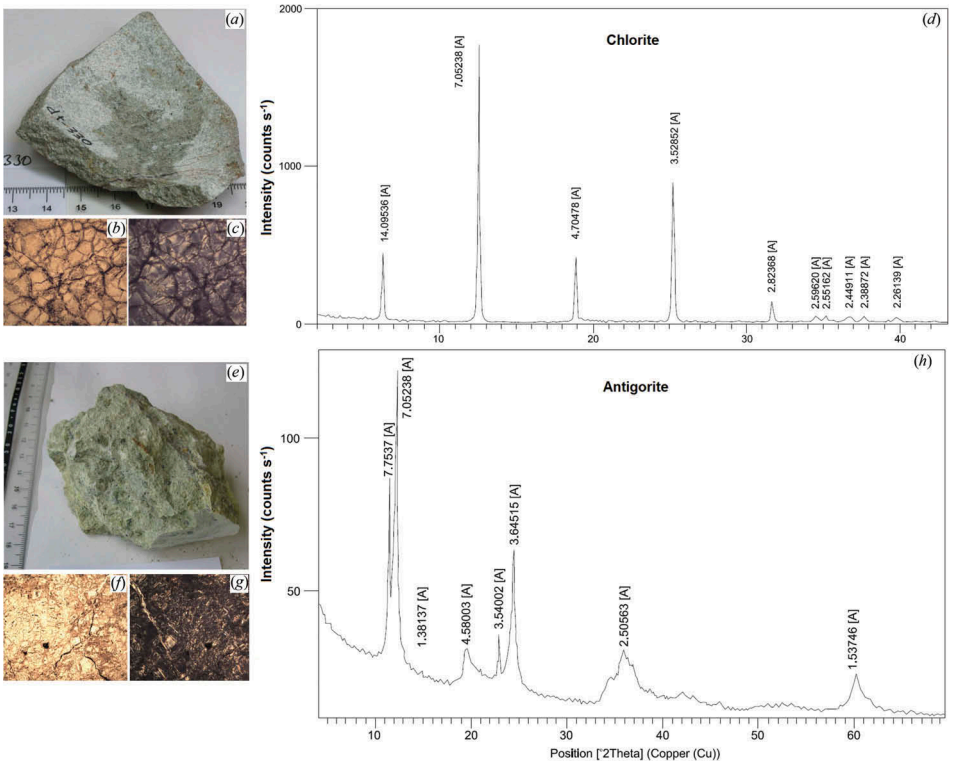

Figure 11. For a representative stone bowl sample views of (*a*) hand specimen, (*b*) thin section with ×4 and PP, (*c*) thin section with ×4 and XP, (*d*) XRD diffractogram and for a representative field sample views of (*e*) hand specimen, (*f*) thin section with ×4 and PP, (*g*) thin section with ×4 and XP, (*h*) XRD diffractogram.

provenance analysis. Nb, La, Ce, Pr, Zr, and Y which are shown in Table 2 are identified as the most discriminating elements and their Normal Mid-Ocean Ridge Basalt (N-MORB) normalized concentrations in the stone bowl and field samples are plotted on the variation diagram by Pearce (1983) and reviewed by Sun and McDonough (1989) as shown in Figure 12. This figure shows that the second petrographic group of stone bowl samples has similar geochemical signatures with the field samples, both having ultramafic petrographic characteristics. On the other hand, there is a second group of stone bowl samples which are geochemically dissimilar to the field samples. These artefact samples belong petrographically to mafic (gabbroic-basaltic) igneous rock types of raw material sources which are not detected as a target area by remote-sensing method applied during this study and sampled during the field studies carried out within the study area (Dirican, Türkmenoğlu, and Atakuman 2016).

5. Conclusion

This study indicates that remote-sensing methods have a significant potential in the identification of source rock locations utilized in the production of archaeological artefacts, such as the stone bowls of Domuztepe. The mineralogical composition of

Table 2. Some trace and rare earth element compositions of stone bowl and field samples.

	Sample	Nb	La	Ce	Pr	Zr	Y		Sample	Nb	La	Ce	Pr	Zr	Y
Stone bowl fragments	S1	0.90	0.24	0.07	0.05	0.16	0.52	Field samples	S48	1.55	0.36	0.08	0.09	0.01	0.01
	S2	0.82	0.36	0.07	0.04	0.19	0.44		S49		0.32	0.05	0.07		0.01
	S3	0.58	0.44	0.15	0.09	0.33	0.34		S50	0.17	0.12		0.02		0.01
	S4	4.85	1.84	1.92	1.72	1.11	2.18		S51	0.30	0.36	0.05	0.05	0.01	0.01
	S5	8.58	2.84	1.71	1.05	1.39	2.98		S52	0.26	0.60	0.19	0.10	0.01	0.01
	S6	1.97	0.60	0.35	0.27	0.50	2.19		S53	0.13	0.28	0.07	0.05	0.01	0.01
	S7	3.26	0.28	0.20	0.09	0.41	0.39		S54	1.12	0.40	0.05	0.06	0.01	
	S8	2.49	3.36	1.92	1.22	0.54	0.36		S55	0.34	0.40	0.07	0.05	0.01	0.01
	S9	2.53	1.68	0.99	0.61	0.29	0.10		S56	0.26	0.40	0.01	0.03	0.01	0.01
	S10	4.16	0.32	0.11	0.10	0.99	1.34		S57	0.09	0.16	0.01	0.02		
	S11	12.32	7.04	3.75	1.98	1.62	0.23		S58	0.09	0.12	0.03			0.01
	S12	0.99	0.36	0.17	0.08	0.18	0.40		S59	0.09	0.12	0.03		0.01	0.01
	S13	0.17	0.24	0.08	0.03	0.03	0.04		S60		0.52	0.05	0.05	0.01	
	S14	1.72	0.36	0.20	0.09	0.47	1.21		S61		0.44	0.15	0.06	0.02	0.01
	S15	0.43	0.84	0.48	0.33	0.12	0.34		S62		0.24		0.05	0.01	0.01
	S16	0.73	18.48	6.39	3.44	0.34	0.25		S63	0.43	0.40	0.05	0.06	0.01	0.02
	S17		0.32	0.05	0.03	0.01	0.02		S64	0.30	0.60	0.07	0.04	0.02	0.01
	S18	0.86	0.60	0.55	0.39	0.27	0.43		S65	0.09	0.36	0.15	0.10	0.01	
	S19	0.64	0.36	0.16	0.08	0.14	0.82		S66	0.94	2.72	2.48	2.29	1.85	1.52
	S20	0.56	0.24	0.11	0.09	0.14	0.30		S67	1.67	10.5	7.24	4.58	1.43	0.63
	S21	0.60	0.16	0.07	0.03	0.16	0.40		S68	1.46	2.24	2.09	1.89	1.70	1.15
	S22	0.64	0.24	0.07		0.22	0.35		S69	0.09	0.24	0.11	0.06	0.04	0.01
	S23	1.33	0.28	0.25	0.21	2.84	0.48		S70		0.56	0.01	0.05	0.01	0.01
	S24	5.45	5.16	3.53	2.58	1.52	0.65		S71		0.48	0.03	0.05	0.02	
	S25	0.64	0.88	0.11	0.04	0.12	0.14		S72	0.09	0.40	0.11	0.10	0.02	0.03
	S26	1.24	0.44	0.09	0.06	0.34	1.03		S73		0.32	0.07	0.07	0.02	
	S27	24.59	26.80	17.43	11.23	3.56	1.90		S74	0.04	0.44	0.05	0.05		
	S28	19.40	8.12	3.72	2.39	4.36	1.01		S75		0.36	0.11	0.05	0.01	
	S29	1.07	1.52	0.75	0.30	0.27	0.48		S76		0.36	0.05	0.02	0.01	
	S30	0.09	0.24	0.08	0.03	0.04	0.01		S77		0.28		0.04	0.01	0.01
	S31	16.61	1.40	0.75	0.42	4.69	0.88		S78		0.52	0.19	0.14	0.01	0.04
	S32		0.20	0.04		0.03			S79	0.09	1.68	1.28	0.90	0.06	0.03
	S33	10.34	0.60	0.47	0.32	2.09	0.38		S80		0.28	0.04	0.05	0.01	0.01
	S34	44.46	46.88	27.19	17.23	6.79	2.73		S81		0.12	0.04	0.02		0.01
	S35	1.07	0.40	0.11	0.05	0.13	0.11		S82		0.08	0.01			
	S36	0.17	0.24	0.07	0.06	0.02	0.03		S83			0.03		0.01	
	S37	0.99	10.52	2.68	0.89	0.20	0.54		S84	0.09	0.08	0.07		0.03	0.02

(*Continued*)

Table 2. (Continued).

Sample	Nb	La	Ce	Pr	Zr	Y	Sample	Nb	La	Ce	Pr	Zr	Y
S38	0.69	0.24	0.05	0.03	0.13	0.36							
S39	0.13	0.16	0.03		0.01	0.01							
S40	0.09	0.12	0.04	0.02	0.01	0.01							
S41	0.77	1.84	0.67	0.33	0.11	0.18							
S42	0.30	0.32	0.13	0.11	0.45	0.79							
S43	1.03	0.12	0.04	0.03	0.19	0.03							
S44	18.93	24.32	12.99	6.91	4.02	1.43							
S45	0.64	0.16	0.04		0.19	0.45							
S46	22.62	0.48	0.32	0.23	1.05	0.65							
S47	0.39	0.16	0.05	0.02	0.06	0.01							

These elements are selected as the most discriminating elements and their N-MORB normalized concentrations in the stone bowl and field samples are plotted on the variation diagram by Pearce (1983) and reviewed by Sun and McDonough (1989) as shown in Figure 12.

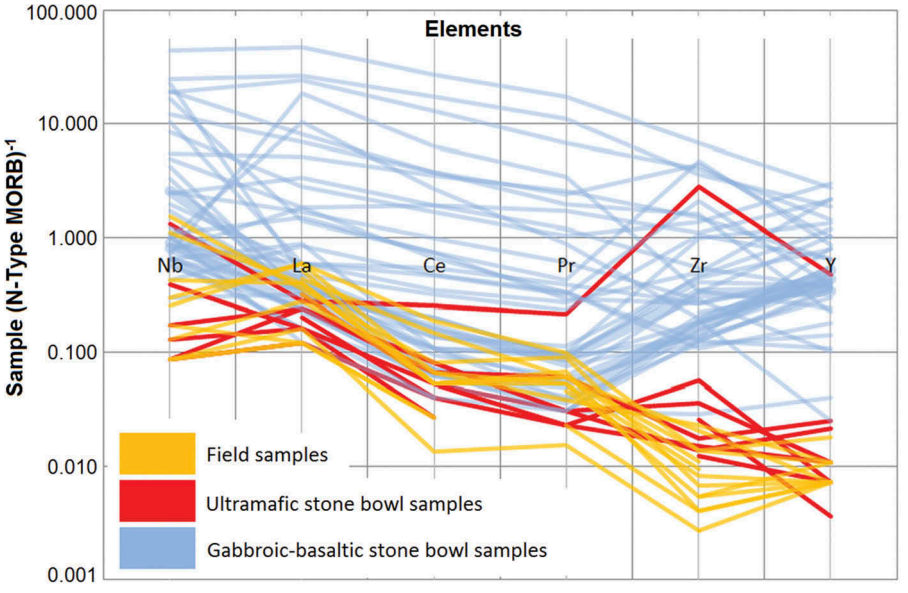

Figure 12. N-MORB-normalized multi-element diagram showing compositions of the ultramafic and mafic (gabbroic-basaltic) rocks as field and stone bowl samples (Pearce 1983; Sun and McDonough 1989).

stone bowls unearthed in Domuztepe showed that the source rocks involved iron-rich chlorite which was then mapped by using ASTER images. However, due to the overlapping spectral features, detection of iron-rich chlorite was a problematic task, especially working with ASTER, since it has limited bands in SWIR where characteristic absorption features are detected. Therefore, instead of performing a single method, three different methods were applied together for the detection of iron-rich chlorite; each of these methods functioned as a filtering mechanism for the other. Band ratioing and feature-selected principle component analysis are applied with an integrated method and later the results are put into a binary image. Relative absorption band-depth images are produced and the possible target areas are compared with the previous binary map. As a combined evaluation of these maps, the most possible target areas are defined. The field study conducted for the validation of applied approach shows that in the target areas the rock samples including iron-rich chlorite are satisfactorily found.

Petrographic-mineralogical and geochemical analysis indicated that for the manufacture of stone vessel samples at least two different raw material sources were utilized: The first group of raw materials is composed of chloritized ultramafic rocks exposed as a part of the ophiolitic units. The second raw material source comprises a mafic igneous rock outcrop. Whereas the first group of raw materials is sampled in the vicinity of Domuztepe, the second group of raw materials has not been found in the field surveys. The data regarding the geochemical signatures of these two groups indicate a genetic relation. Therefore, it is concluded that the source rock of a major portion of the stone bowls unearthed at Domuztepe most probably originated from the near vicinity of the site although the exact location of the Fe-chlorite rich ultramafic rock source(s) could not be located. It is also concluded that based on the abundance of ultramafic rock sources in the near vicinity

of Domuztepe site, the ultramafic stone bowl artefacts are locally produced. This study also indicates that gabbroic-basaltic stone bowl samples have raw material sources located further away from Domuztepe site and transported to the site by trading.

Acknowledgements

We would like to thank Prof. Dr Stuart Campbell and Prof. Dr Elizabeth Carter, the project leaders of the excavations at Domuztepe and Kahramanmaraş Archaeology Museum, for the access to the prehistoric stone vessel pieces from the site. We acknowledge Assos. Prof. Dr Kaan Sayıt for his helps in processing the geochemical data and Dr Arda Arcasoy for his helps in spectral analyses of stone bowls. This study was partly supported by the Scientific and Technological Research Council of Turkey (TÜBİTAK, Grant No: YDABÇAG-112Y135).

Disclosure statement

No potential conflict of interest was reported by the authors.

Funding

This study was partly supported by the Scientific and Technological Research Council of Turkey [TÜBİTAK, Grant No: YDABÇAG-112Y135].

References

Abrams, M., S. Hook, and B. Ramachandran. 2002. "ASTER User Handbook, Version 2." *NASAJet Propulsion Laboratory* 4800: 135.

Ben-Dor, E., F. A. Kruse, A. B. Lefkoff, and A. Banin. 1995. "Comparison of Three Calibration Techniques for Utilization of GER 63-Channel Aircraft Scanner Data of Makhtesh Ramon, Negev, Israel." *International Journal of Rock Mechanics and Mining Sciences & Geomechanics Abstracts*, 32 (4): A164, doi:10.1016/0148-9062(95)97031-D.

Bishop, J. L., M. D. Lane, M. D. Dyar, and A. J. Brown. 2008. "Reflectance and Emission Spectroscopy Study of Four Groups of Phyllosilicates: Smectites, Kaolinite-Serpentines, Chlorites and Micas." *Clay Minerals* 43 (1): 35–54. doi:10.1180/claymin.2008.043.1.03.

Brandmeier, M., S. Erasmi, C. Hansen, A. Höweling, K. Nitzsche, T. Ohlendorf, M. Mamani, and G. Wörner. 2013. "Mapping Patterns of Mineral Alteration in Volcanic Terrains Using ASTER Data and Field Spectrometry in Southern Peru." *Journal of South American Earth Sciences* 48: 296–314. doi:10.1016/j.jsames.2013.09.011.

Campbell, B. 2012. "Stone Bowls in the Halaf: Manufacture, Function and Breakage at Domuztepe." In *Interpreting the Late Neolithic of Upper Mesopotamia*, edited by O. P. Nieuwenhuyse, R. Bernbeck, P. M. M. G. Akkermans, and J. Rogasch, 241–250, Brepols.

Campbell, S., and E. Carter. 1998. *Excavations at Domuztepe 1997, Kazi Sonuclari Toplantisi 20*, 283–294. Ankara: TC Kültür ve Turism Bakanliği, Kültür Varliklari ve Müzeler Genel Müdürlüğü.

Campbell, S., E. Carter, E. Healey, S. Anderson, A. Kennedy, and S. Whitcher. 1999. "Emerging Complexity on the Kahramanmaraş Plain, Turkey: The Domuztepe Project, 1995-1997." *American Journal of Archaeology* 103: 395–418. doi:10.2307/506968.

Carter, E., S. Campbell, and S. Gauld. 2003. "Elusive Complexity: New Data from Late Halaf Domuztepe in South Central Turkey." *Paléorient* 29 (2): 117–133.

Clark, B. C., R. E. Arvidson, R. Gellert, R. Van Morris, D. W. Ming, L. Richter, S. W. Ruff, J. R. Michalski, W. H. Farrand, and A. Yen. 2007. "Evidence for Montmorillonite or Its Compositional Equivalent

in Columbia Hills, Mars." *Journal of Geophysical Research: Planets* 112: E6. doi:10.1029/2006JE002756.

Crosta, A. P., C. R. De Souza Filho, F. Azevedo, and C. Brodie. 2003. "Targeting Key Alteration Minerals in Epithermal Deposits in Patagonia, Argentina, Using ASTER Imagery and Principal Component Analysis." *International Journal of Remote Sensing* 24 (21): 4233–4240. doi:10.1080/0143116031000152291.

Crosta, A. P., and J. M. C. M. Moore. 1990. "Enhancement of Landsat Thematic Mapper Imagery for Residual Soil Mapping in SW Minas Gerais State, Brazil- A Prospecting Case History in Greenstone Belt Terrain." Paper presented at the Thematic Conference on Remote Sensing for Exploration Geology- Methods, Integration, Solutions, 7th, Calgary, Canada.

Crowley, J. K., D. W. Brickey, and L. C. Rowan. 1989. "Airborne Imaging Spectrometer Data of the Ruby Mountains, Montana: Mineral Discrimination Using Relative Absorption Band-Depth Images." *Remote Sensing of Environment* 29 (2): 121–134. doi:10.1016/0034-4257(89)90021-7.

Cudahy, T., M. Jones, M. Thomas, C. Laukamp, M. Caccetta, R. Hewson, A. Rodger, and M. Verrall. 2008. "Next Generation Mineral Mapping: Queensland Airborne Hymap and Satellite ASTER Surveys 2006–2008: Perth." *Publicly Available Report P* 2007. Queensland: CSIRO Exploration and Mining.

Cudahy, T. J., K. Okada, A. Cornelius, and R. D. Hewson. 2002. "Regional to Prospect Scale Exploration for Porphyry-Skarn-Epithermal Mineralisation at Yerington, Nevada, Using ASTER and Airborne Hyperspectral Data." CSIRO Exploration and Mining Report. CSIRO, Kensington.

Dalton, J. B., D. J. Bove, C. S. Mladinich, and B. W. Rockwell. 2004. "Identification of Spectrally Similar Materials Using the USGS Tetracorder Algorithm: The Calcite–Epidote–Chlorite Problem." *Remote Sensing of Environment* 89 (4): 455–466. doi:10.1016/j.rse.2003.11.011.

Dirican, M., A. Türkmenoğlu, and Ç. Atakuman. 2016. *Domuztepe'nin (Kahramanmaraş) Taş Kapları, 4. ODTÜ Arkeometri Çalıştayı Bildiriler Kitabı: Türkiye Arkeolojisinde Taş: Arkeolojik Ve Arkeometrik Çalışmalar - Prof. Dr. Hayriye Yeter Göksu Onuruna*. Ankara: Bilgin Kültür Sanat Yayınları.

ITT. 2010. *ENVI 4.8 Software*. White Plains, NY: ITT Corporation.

Kansa, S. W., S. C. Gauld, S. Campbell, and E. Carter. 2009. "Whose Bones are Those? Preliminary Comparative Analysis of Fragmented Human and Animal Bones in the "Death Pit" at Domuztepe, a Late Neolithic Settlement in Southeastern Turkey." *Anthropozoologica* 44 (1): 159–172. doi:10.5252/az2009n1a7.

Lasaponara, R., and N. Masini. 2009. "Special Issue on "Remote Sensing for Cultural Heritage Management and Documentation"." *Journal of Cultural Heritage* 10: e1–e2. doi:10.1016/j.culher.2009.10.006.

Loughlin, W. P. 1991. "Principal Component Analysis for Alteration Mapping." *Photogrammetric Engineering and Remote Sensing* 57 (9): 1163–1169.

MicroImages. 1997. "TNTmips." http://www.microimages.com

Moore, D. M., and J. R. C. Reynolds. 1997. *X-Ray Diffraction and the Identification and Analysis of Clay Minerals*, 378. New York: Oxford University Press.

MTA. 2004. *MTA 1/500000 Geological Map of Turkey*. Ankara: MTA.

Orlando, P., and B. de Villa. 2011. "Remote Sensing Applications in Archaeology." *Archeologia E Calcolatori* 22: 147–168.

Öztan, S. N., and M. L Süzen. 2011. "Mapping Evaporate Minerals by ASTER." *International Journal of Remote Sensing* 32 (6): 1651–1673. doi:10.1080/01431160903586799.

Parcak, S. H. 2009. *Satellite Remote Sensing for Archaeology*. New York: Taylor & Francis Group.

Pazand, K., J. F. Sarvestani, M. Reza, and S. Ravasan. 2013. "Hydrothermal Alteration Mapping Using ASTER Data for Reconnaissance Porphyry Copper Mineralization in the Ahar Area, NW Iran." *Journal of the Indian Society of Remote Sensing* 41 (2): 379–389. doi:10.1007/s12524-012-0229-0.

Pearce, J. A. 1983. *Role of the Sub-Continental Lithosphere in Magma Genesis at Active Continental Margins*. In *Continental basalts and mantle xenoliths,* edited by C. J. Hawkesworth, and M. J. Norry, 230-249, Nantwich, Cheshire: Shiva Publications.

Pour, A. B., and M. Hashim. 2012. "The Application of ASTER Remote Sensing Data to Porphyry Copper and Epithermal Gold Deposits." *Ore Geology Reviews* 44: 1–9. doi:10.1016/j.oregeorev.2011.09.009.

Prost, G. L. 2013. *Remote Sensing for Geoscientists: Image Analysis and Integration*. Florida: CRC Press.

Robb, L. 2013. *Introduction to Ore-Forming Processes*. Malden, USA: Blackwell Publishing company.
Rowan, L. C., S. J. Hook, M. J. Abrams, and J. C. Mars. 2003. "Mapping Hydrothermally Altered Rocks at Cuprite, Nevada, Using the Advanced Spaceborne Thermal Emission and Reflection Radiometer (ASTER), a New Satellite-Imaging System." *Economic Geology* 98 (5): 1019–1027. doi:10.2113/gsecongeo.98.5.1019.
Rowan, L. C., R. G. Schmidt, and J. C. Mars. 2006. "Distribution of Hydrothermally Altered Rocks in the Reko Diq, Pakistan Mineralized Area Based on Spectral Analysis of ASTER Data." *Remote Sensing of Environment* 104 (1): 74–87. doi:10.1016/j.rse.2006.05.014.
Salisbury, J. L. 1983. "Contractile Flagellar Roots: The Role of Calcium." *Journal Submicrosc Cytological* 15: 105–110.
Sever, T. L. 1995. "Remote-Sensing." *American Journal of Archaeology* 99 (1): 83–84.
Sun, -S.-S., and WF-s. McDonough. 1989. "Chemical and Isotopic Systematics of Oceanic Basalts: Implications for Mantle Composition and Processes." *Geological Society, London, Special Publications* 42 (1): 313–345. doi:10.1144/GSL.SP.1989.042.01.19.
Williamson, R. A., and P. R. Nickens. 2000. *Science and Technology in Historic Preservation*. 4vols. New York: Springer Science & Business Media.
Yilmaz, H., S. Over, and S. Ozden. 2006. "Kinematics of the East Anatolian Fault Zone between Turkoglu (Kahramanmaras) and Celikhan (Adiyaman), Eastern Turkey." *Earth, Planets and Space* 58 (11): 1463–1473. doi:10.1186/BF03352645.